BOLETÍN DE LA SOCIEDAD ESPAÑOLA DE CERÁMICA Y VIDRIO XXX (XXXX) 100477

BOLETIN DE LA SOCIEDAD ESPAÑOLA DE
Cerámica y Vidrio
www.elsevier.es/bsecv

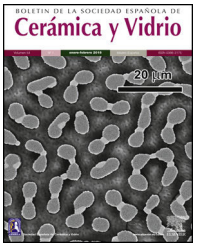

Original

Archaeometric analysis of Nasrid glazed architectural ceramics from the Alhambra and Generalife Monument, Granada (Spain)

Carolina Cardell[a], Maja Urosevic[a,*], Danielle Dias Martins[b], Isabel Guerra[c], Alberto García Porras[b]

[a] Department of Mineralogy & Petrology, Faculty of Science, University of Granada, 18071 Granada, Spain
[b] Department of Medieval History and Historiographic Sciences and Techniques, Faculty of Arts, University of Granada, 18071 Granada, Spain
[c] Scientific Instrumentation Centre. University of Granada, Campus Universitario Fuentenueva, 18071 Granada, Spain

ARTICLE INFO

Article history:
Received 10 June 2025
Accepted 12 November 2025
Available online xxx

Keywords:
Archaeometry
Architectural ceramics
Glaze
Chromophores
Al-Andalus

ABSTRACT

This work presents the first systematic archaeometric data of 13th–14th century AD Nasrid glazed architectural ceramics from the Alhambra and Generalife, focusing on colour-specific glazing technologies. Findings provide new insights into Nasrid glazing technology, ceramic typologies, and conservation implications, contributing to discussions on Islamic material culture and technical traditions in al-Andalus. Analysed typologies include mosaic, inlay, relief tiles, roof lights, and steles with glazes in white, blue, green-turquoise, black, and honey tones. Microstructural and chemical results reveal decorative chromophores and techniques to be a reference for future studies. Most glazes are inglaze on lead tin-opacified bases, fired in oxidising conditions at ~950 °C. Phosphorus was found in weathered glazes (associated with a burial environment) and unweathered white and blue glazes, suggesting deliberate addition of bones (fragments/ashes). Identified phases in most glazes were unmelted quartz and feldspars grains, and relatively abundant Cr-bearing wollastonite crystals precipitated during firing. Furthermore, one of the fragments with a black surface was determined not to be a glaze, but rather a polished section of a metamorphic rock.

* *Corresponding author.*
E-mail address: maja@ugr.es (M. Urosevic).
https://doi.org/10.1016/j.bsecv.2025.100477

Please cite this article in press as: C. Cardell, et al., Archaeometric analysis of Nasrid glazed architectural ceramics from the Alhambra and Generalife Monument, Granada (Spain), Bol. Soc. Esp. Cerám. Vidr. (2025), https://doi.org/10.1016/j.bsecv.2025.100477

Análisis arqueométrico de cerámicas vidriadas arquitectónicas nazaríes del Complejo monumental de la Alhambra y Generalife, Granada (España)

Palabras clave:
Arqueometría
Cerámica arquitectónica
Esmalte
Cromóforos
Al-Andalus

RESUMEN

Este trabajo presenta datos del primer análisis arqueométrico sistemático de cerámicas vidriadas arquitectónicas de los siglos XIII y XIV n.e. de la Alhambra y Generalife, centrándose en la tecnología de esmaltado de diversos colores. Los resultados ofrecen nuevas perspectivas sobre la tecnología del vidriado nazarí, las tipologías cerámicas y su estado de conservación. Estos hallazgos permiten abordar una discusión más amplia de la cultura material islámica y de las tradiciones técnicas de al-Andalus. Las tipologías cerámicas estudiadas incluyen alicatados, incrustados, sebkas, lucernarios y bordillos funerarios coloreados en blanco, azul, verde-turquesa, negro y melado. Los resultados microestructurales y químicos revelan que los cromóforos y técnicas decorativas en determinados tipos cerámicos pueden servir como marcadores en estudios futuros. Los esmaltes son de plomo opacificados con estaño, y cocidos en atmósfera oxidante a unos 950 °C. Se detectó fósforo en muestras alteradas (relacionado con condiciones de enterramiento), y en esmaltes blancos y azules no alterados, lo que sugiere la adición deliberada de huesos o cenizas óseas al vidriado. Asimismo, se identificaron en la mayoría de los esmaltes granos de cuarzo y feldespatos no fundidos, y abundantes precipitados de wollastonita con trazas de cromo. Además, se determinó que uno de los fragmentos con decoración negra no era un vidriado, sino una sección pulida de una roca metamórfica.

Introduction

Archaeometric studies of glazed ceramics have achieved significant maturity, employing a range of analytical techniques to yield insights into ancient manufacturing processes, chromophores, and degradation mechanisms [1–11]. Quantitative assessments of glaze constituents, coupled with analyses of refractory and crystallisation phases, and structure and morphology examination of the glaze–ceramic interface, offer significant information [2,7,12]. Analyses reveal details of manufacturing processes such as firing temperature, atmospheric firing conditions, firing stage sequences, and colour techniques [7,9,10]. Data provide historical insights, including trade or local sourcing of raw materials, adaptation of foreign techniques, aesthetic evolution [13], and likewise strategies for conservation and restoration.

Architectural ceramics, compared with tableware ceramics [1–4,8,9,14,15], are not as extensively analysed, although studies have been conducted in Portugal [5,16], Spain [11,17,18], Mesopotamia and Middle-East regions [19,20]. Noteworthy are the Nasrid architectural ceramics, specifically from the Alhambra and Generalife [21,22]. The Nasrid period refers to the era between AD 1232 and 1492 during which the Nasrid dynasty ruled the Granada Emirate, the last Muslim state in the Iberian Peninsula. The Alhambra architectural ceramics have been studied by historians and archaeologists [21,23]. However, their analysis remains challenging because the monument dimension, unrecorded relocations of ceramic pieces, undocumented and Christian interventions, and chronologies based on artistic and stylistic features. Chronologies need reassessment considering archaeometric and interdisciplinary investigations. Today archaeometric studies of Nasrid glazed architectural ceramics are still emerging and remains non-systematic [17,21,24–29]. However, most recent results reveal their lead tin-opacified composition [7,28].

This study is part of an interdisciplinary research and presents a morphological and chemical analysis of coloured glazed architectural ceramics from the Alhambra and Generalife dated on 13th–14th century AD according to decoration [30]. The aim is to improve knowledge on their chronology and technology of fabrication.

Materials and methods

Materials

Thirteen architectural ceramic pieces from key locations within the Alhambra and Generalife (Figs. 1 and 2, Table 1, Table S1 and Appendix 1) featuring geometric patterns, vegetal motifs and Arabic calligraphy, were studied. Pieces are housed in the Museum's private storage of the Alhambra. Information for each piece is recorded in the *Integrated Museum Documentation and Management System* (DOMUS [22]) of the monument (Table 1 and Table S1). Pieces exhibit white, blue, green-turquoise, black and honey colour, and correspond to *Alicatado* (mosaic tiling), *Incrustado* (inlay tiles), *Lucernario* (rooflight fragments), *Sebka* (relief tiles), and *Bordillo* (funerary steles), illustrating diverse functions (Table S1).

Analytical techniques

A stereomicroscope (Leica VDM 2000) documented macroscopic features of samples (Fig. 3). Samples were embedded within epoxy mounts and polished to achieve cross-sections. Mineralogical and microstructural analyses were performed

Please cite this article in press as: C. Cardell, et al., Archaeometric analysis of Nasrid glazed architectural ceramics from the Alhambra and Generalife Monument, Granada (Spain), Bol. Soc. Esp. Cerám. Vidr. (2025), https://doi.org/10.1016/j.bsecv.2025.100477

Table 1 – Characteristics of studied glazed architectural ceramics from the Alhambra and Generalife.

Map reference[a]	Domus[b] reference code	Tipology	Technique	Ceramic glaze colours	Glaze colour and code sample	Use/purpose	Minerals detected in the glaze[c]
13th century AD							
1	A085786/19	Tile	Inlay	Green-Turquoise	Green-Turquoise: A085786/19_GT	Ceramic screed element or wall cladding	GT: Diopside, SnO_2
1	A085786/20	Tile	Inlay	White, Black	White: A085786/20_W	Wall cladding. Ceramic plinth	W: SnO_2, (albite)
1	A085786/25	Rooflight (*Lucernario*)	Painted	White	White: A085786/25_W	Lighting of rooms	W: Diopside, wollastonite, apatite, SnO_2, (quartz, Na–Ca plagioclase)
1	A085786/38+B4:B7	Rooflight (*Lucernario*)	Painted	Blue	Blue: 085786/38_BL	Lighting of rooms	BL: Diopside, wollastonite, apatite, SnO_2, (quartz, albite)
2	91288	Tiling mosaic panel	Tiling mosaic	White, Black	Black: 91288_BK	Wall cladding. Ceramic plinth	BK: strongly weathered
2	91290	Tiling mosaic panel	Tiling mosaic	White, Black	White: 91290_W	Wall cladding. Ceramic plinth	W: Diopside, SnO_2, (quartz)
3	121708	Tile	Inlay	Green-Turquoise	Green-Turquoise: 121708_GT	Arch soffit. Voussoir	GT: Wollastonite, SnO_2
4	124965	Tiling mosaic panel	Tiling mosaic	White, Blue, Green-Turquoise, Black	White: 124965_W Blue: 124965_BL Green-Turquoise: 124965_GT	Wall cladding	W: SnO_2; BL: Diopside, SnO_2; GT: none
14th century AD							
5	1294	Tile	Inlay	White, Blue	White: 1294_W Blue: 1294_BL	Wall cladding. Framing of a plinth	W: SnO_2, (Al_2SiO_5, orthoclase, quartz); BL: Wollastonite; SnO_2
6	1319	Funerary stele	Painted	White, Blue	White: 1319_W Dark Blue: 1319_DBL Light Blue: 1319_LBL	Gravestone	W: Ca-feldspar, SnO_2, (quarzt); DBL: Wollastonite, Fe–Co-rich inclusion, franklinite-magnetite-spinel, (quartz); LBL: SnO_2, (quartz)
7	1382	Tiling mosaic panel	Tiling mosaic	White, Black, Honey	White: 1382_W Black: 1382_BK Honey: 1382_H	Wall cladding. Ceramic plinth	W: Wollastonite, (quartz); BK: Rock fragment (metapelite); H: Cr-bearing wollastonite
8	2264	Tiling mosaic panel	Tiling mosaic	White, Green-Turquoise, Black, Honey	White: 2264_W Green-Turquoise: 2264_GT Black: 2264_BK Honey: 2264_H1, 2264_H2	Wall cladding. Ceramic plinth	W: SnO_2; GT: Cr-bearing wollastonite, SnO_2; H: Ilmenite, K-feldspar, Ca–K–feldspar; H1: SnO_2, (quartz)
9	132766	Tile	Relief	Blue, Green-Turquoise	Blue: 132766_BL Green-Turquoise: 132766_GT	Arch and door cladding (*sebka*)	BL: Diopside, wollastonite, SnO_2, Ca-Pb-P phase, (quartz)

[a] See Fig. 1 for original ceramic location in the monument.
[b] Integrated Museum Documentation and Management System.
[c] In parenthesis mineral interpreted as unmelted phase.

Please cite this article in press as: C. Cardell, et al., Archaeometric analysis of Nasrid glazed architectural ceramics from the Alhambra and Generalife Monument, Granada (Spain), Bol. Soc. Esp. Cerám. Vidr. (2025), https://doi.org/10.1016/j.bsecv.2025.100477

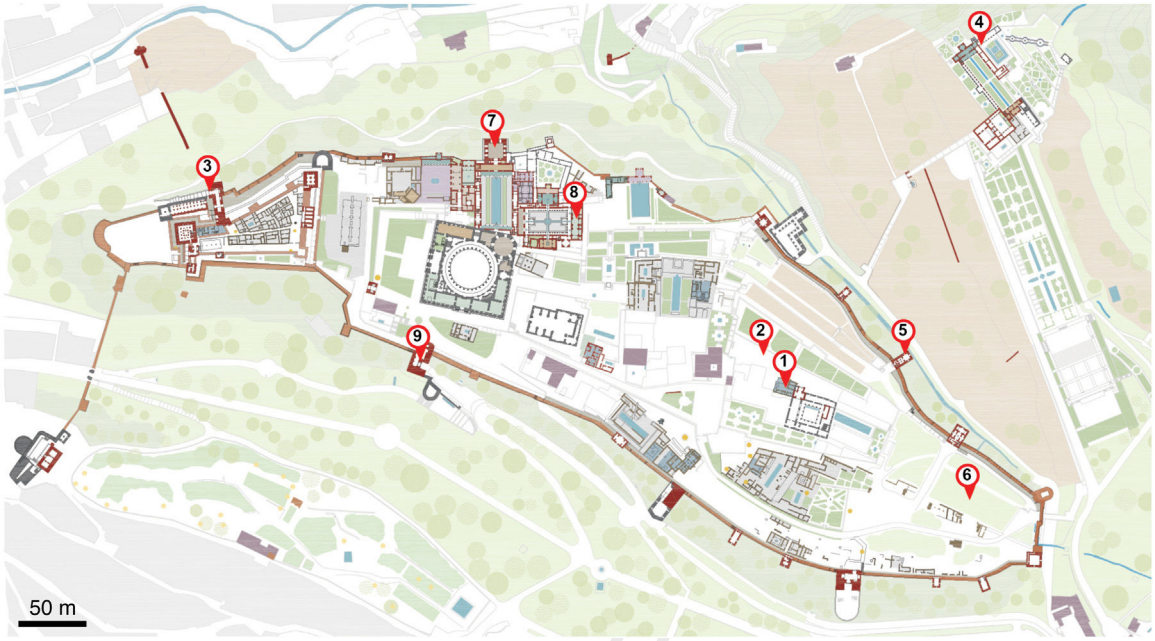

Fig. 1 – Map of the Alhambra and Generalife Monument (Granada, Spain) with the original location of the studied glazed ceramics; site 1: Bath of the Monastery of San Francisco (archaeological site); site 2: Garden of the Monastery of San Francisco (archaeological site), site 3: Gate of the Arms; site 4: Generalife; site 5: Tower of the Captive; site 6: City of the Alhambra (Medina); site 7: Hall of the Kings at the Lion Palace, site 8: Gate of Justice.
Map from the Alhambra and Generalife Council, amended by Dias Martins.

employing a Carl Zeiss Jenapol-U polarised optical microscope (OM), coupled to a Nikon D7000 digital camera. Observations encompassed transmitted and reflected light under plane and cross-polarised conditions.

High-resolution backscattered electron (BSE) and secondary electron (SE) imaging were acquired from carbon-coated thin sections under a high vacuum using two scanning electron microscopes (SEM). A field emission environmental SEM (FE-ESEM) QuemScan 650F equipped with a CBS detector for BSE. By using a Dual EDS XFlash of Bruker with a XFlash 6/30 detector, EDS microanalyses and elemental maps were obtained in selected point and areas respectively. Also, a Zeiss SUPRA40VP FE-SEM was used, equipped with X-Max 50 mm^2 EDS detector (AZTEC v.3), enabling point and surface analyses, and compositional mapping. Quantitative analyses (normalised) were obtained using AZTEC certified pure element and compound standards (Table S2).

Chemical characterisation began with low-magnification BSE imaging, including the glaze and ceramic body, and to identify pristine and weathered glaze regions. Inferred original glaze composition was estimated through surface analyses of three to five regions (from ca. 150×100 to $70 \times 50\,\mu m^2$), using 15 kV accelerating voltage and 8.5 mm working distance. Average composition of areas was reported as oxides (weight %). Measurement reliability was ensured by evaluating the distribution homogeneity of quench materials. The surface measured by EDS mapping is representative for Sn based on the small size (<1 μm) and homogenous distribution of SnO_2, but it might underestimate the amount of Ca, Mg, Si and P, based on larger size and non-homogeneous distribution of pyroxene, wollastonite and apatites.

EDS single-point analyses were conducted in crystal precipitates and unmelted crystals. Complex phases were validated through stoichiometric calculations). Subsequent BSE imaging of glaze–ceramic interfaces was done to investigate chemical reactions and diffusion processes. X-ray maps (1024×768 pixels, 10 ms dwell time, 2.5 h acquisition, 20 eV/channel resolution) were acquired from areas of interest.

Results and discussion

Chemical data are presented according to glaze colours (Table 2) to discern recipes according to ceramic typology or chronology, and to determine ceramic reference groups. Note that the 13th century AD ceramics from the Monastery of San Francisco (Table S1) are considered original Nasrid pieces and they have never been intervened. Hence, their characteristics are a benchmark of this period. Comparison of Nasrid glazes' compositions with contemporaneous architectural ceramics is limited due to the scarcity of relevant bibliographic sources (see Table S3 for compositional data on comparable coeval coloured glazes).

White glaze

Chemical composition

White glazes exhibit significant compositional variability (Table 2). However, except for the weathered 91290_W glaze, all are classified as lead tin-opacified glazes [2]. Differences

Please cite this article in press as: C. Cardell, et al., Archaeometric analysis of Nasrid glazed architectural ceramics from the Alhambra and Generalife Monument, Granada (Spain), Bol. Soc. Esp. Cerám. Vidr. (2025), https://doi.org/10.1016/j.bsecv.2025.100477

Fig. 2 – Studied glazed ceramic fragments. Codes refer to the Integrated Museum Documentation and Management System (DOMUS) of the Alhambra and Generalife Monument.

Please cite this article in press as: C. Cardell, et al., Archaeometric analysis of Nasrid glazed architectural ceramics from the Alhambra and Generalife Monument, Granada (Spain), Bol. Soc. Esp. Cerám. Vidr. (2025), https://doi.org/10.1016/j.bsecv.2025.100477

Table 2 – Average quantitative EDS analyses (wt.%) of the investigated glazes.

Sample	Class	Century	Tipology	Symbol	Na_2O	MgO	Al_2O_3	SiO_2	P_2O_5	K_2O	CaO	TiO_2	V_2O_5	MnO	Fe_2O_3	CuO	CoO	ZnO	BaO	PbO	SnO_2
91290_W	White	13	Tiling mosaic panel	W	0.37	0.77	1.34	11.01	8.86	0.35	12.46	0.00	0.00	0.00	0.51	0.00	0.00	0.00	0.00	53.45	10.88
A085786/20_W	White	13	Tile	W	2.07	0.00	1.03	35.81	0.00	0.71	2.18	0.00	0.00	0.00	0.52	0.00	0.00	0.00	0.00	50.85	6.85
A085786/25_W	White	13	Rooflight	W	2.88	0.77	1.04	39.99	0.00	2.27	2.67	0.00	0.00	0.00	0.58	0.00	0.00	0.00	0.00	44.11	5.69
124965_W	White	13	Tiling mosaic panel	W	2.90	0.53	0.82	34.56	0.23	1.07	1.59	0.00	0.00	0.00	0.64	0.00	0.00	0.00	0.00	50.90	6.75
1294_W	White	14	Tile	W	1.99	0.00	0.37	36.29	0.00	1.80	2.75	0.00	0.00	0.00	0.63	0.00	0.00	0.00	0.00	46.99	9.18
1382_W	White	14	Tiling mosaic panel	W	1.51	0.32	2.18	32.33	0.00	2.14	1.10	0.00	0.00	0.00	0.63	0.00	0.00	0.00	0.00	43.54	16.24
2264_W	White	14	Tiling mosaic panel	W	3.1	0.62	1.13	34.92	0.00	0.64	1.55	0.00	0.00	0.00	0.60	0.00	0.00	0.00	0.00	53.41	4.03
1319_W	White	14	Funerary stele	W	2.56	0.00	0.50	31.30	0.00	0.76	1.15	0.00	0.00	0.00	0.48	0.00	0.00	0.00	0.00	52.25	9.69
124965_BL	Blue	13	Tiling mosaic panel	BL	2.08	0.73	0.73	35.45	0.00	1.97	2.41	0.00	0.00	0.00	1.62	0.31	0.12	0.33	0.00	47.20	7.06
A085786/38_BL	Blue	13	Rooflight	BL	2.36	0.79	1.09	36.47	0.00	1.58	2.16	0.00	0.00	0.00	1.26	0.00	0.00	0.15	0.00	47.23	6.90
1294_BL	Blue	14	Tile	BL	1.12	0.42	1.22	35.34	0.00	1.87	3.95	0.00	0.00	0.00	2.20	0.16	0.58	0.90	0.00	43.36	8.88
132766_BL	Blue	14	Tile	BL	1.32	0.00	0.77	32.06	0.00	1.41	2.71	0.00	0.00	0.00	1.76	0.14	0.79	0.68	0.00	49.41	8.46
1319_LBL	Blue	14	Funerary stele	BL	2.38	0.00	0.36	31.45	0.00	1.06	0.85	0.00	0.00	0.00	0.24	0.00	0.00	0.00	0.00	54.01	8.75
1319_DBL	Blue	14	Funerary stele	BL	2.11	0.00	0.69	31.02	0.00	1.10	1.33	0.00	0.00	0.00	1.07	0.29	0.00	0.90	0.00	51.03	9.47
124965_GT	Green Turquoise	13	Tiling mosaic panel	GT	2.53	0.76	1.54	41.04	0.00	1.96	3.41	0.00	0.00	0.00	0.79	1.22	0.00	0.00	0.00	42.04	4.73
121708_GT	Green Turquoise	13	Tile	GT	1.80	0.81	2.82	41.91	0.00	1.27	4.35	0.00	0.00	0.00	1.41	2.03	0.00	0.00	0.00	37.51	6.10
A085786/19_GT	Green Turquoise	13	Tile	GT	1.46	1.02	2.05	33.87	0.00	1.12	3.06	0.00	0.00	0.00	1.08	2.06	0.00	0.00	0.00	47.31	6.97
2264_GT	Green Turquoise	14	Tiling mosaic panel	GT	1.10	0.34	6.99	44.03	0.00	2.05	5.32	0.12	0.00	0.00	2.17	1.37	0.00	0.00	0.00	36.03	0.47
132766_GT	Green Turquoise	14	Tile	GT	1.84	0.31	0.42	31.29	0.00	1.21	1.88	0.00	0.00	0.00	0.48	3.50	0.00	0.00	0.00	50.87	8.22
91288_BK_m1	Black	13	Tiling mosaic panel	BK	0.00	3.31	0.00	0.00	0.00	0.00	96.69	0.00	0.00	0.00	0.00	0.00	0.00	0.00	0.00	0.00	0.00
91288_BK_m2	Black	13	Tiling mosaic panel	BK	0.00	0.28	0.27	1.96	3.19	0.00	72.12	0.00	0.00	0.00	0.00	0.00	0.00	0.00	0.00	21.19	0.00
91288_BK_g	Black	13	Tiling mosaic panel	BK	0.00	0.45	1.78	7.14	3.62	0.00	4.09	0.00	0.38	15.01	1.37	0.00	0.00	0.00	0.00	65.24	0.00
1382_BK	Black	14	Tiling mosaic panel	BK	1.89	1.03	35.38	50.52	0.00	8.08	0.00	0.18	0.00	0.00	2.73	0.00	0.00	0.00	0.21	0.00	0.00
2264_BK	Black	14	Tiling mosaic panel	BK	0.40	0.87	6.40	37.76	0.00	1.80	5.85	0.00	0.00	4.74	4.08	0.00	0.00	0.00	1.28	36.83	0.00
1382_H	Honey	14	Tiling mosaic panel	H	0.96	0.53	3.30	32.87	0.00	1.98	3.15	0.22	0.00	0.00	3.15	0.00	0.00	0.00	0.00	53.85	0.00
2264_H1	Honey	14	Tiling mosaic panel	H	2.95	0.45	1.01	34.37	0.00	0.88	1.12	0.00	0.00	0.00	0.53	0.00	0.00	0.00	0.00	53.64	5.04
2264_H2	Honey	14	Tiling mosaic panel	H	0.40	0.31	6.88	42.06	0.00	2.07	5.79	0.00	0.00	0.00	3.17	0.00	0.00	0.00	1.22	38.10	0.00

Please cite this article in press as: C. Cardell, et al., Archaeometric analysis of Nasrid glazed architectural ceramics from the Alhambra and Generalife Monument, Granada (Spain), Bol. Soc. Esp. Cerám. Vidr. (2025), https://doi.org/10.1016/j.bsecv.2025.100477

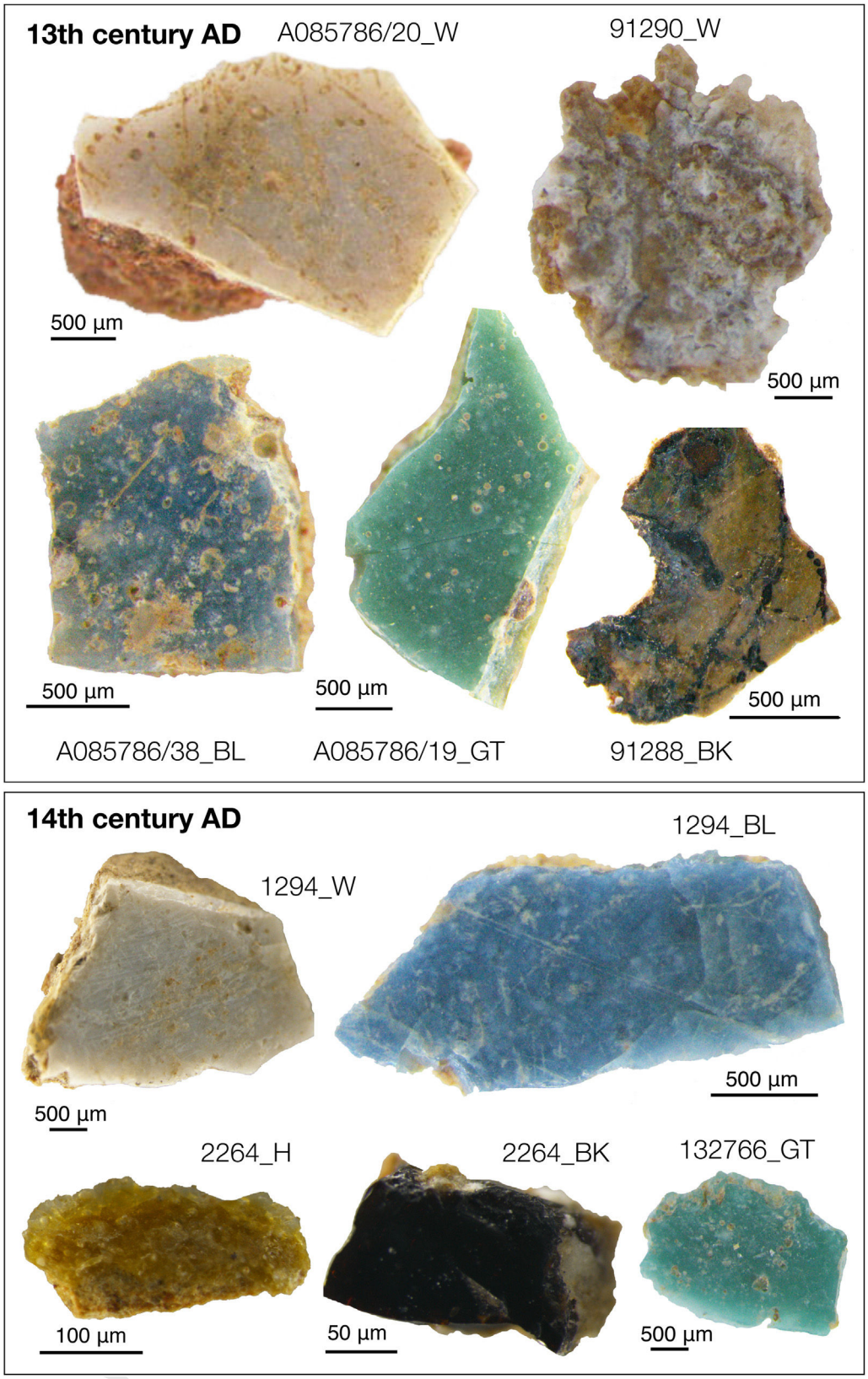

Fig. 3 – Stereomicroscope images of some representative studied architectural glazed ceramics.

Please cite this article in press as: C. Cardell, et al., Archaeometric analysis of Nasrid glazed architectural ceramics from the Alhambra and Generalife Monument, Granada (Spain), Bol. Soc. Esp. Cerám. Vidr. (2025), https://doi.org/10.1016/j.bsecv.2025.100477

in composition are associated with ceramic typology rather than chronology, excluding some 14th century AD pieces, as discussed below.

Tiling mosaic panels

The 13th century AD 124965_W glaze (520 μm thick) has the lowest Al_2O_3 content (0.82 wt.%) compared to the 14th century AD glazes 1382_W (220 μm thick) and 2264_W (330 μm thick), which contain 2.18 and 1.13 wt.%, respectively. Additionally, glaze 124965_W holds phosphorous (P, expressed as P_2O_5 at 0.23 wt.%, Table 2), related to weathering (discussed below) as confirmed by surface pitting and microcracking.

Composition of the 13th century AD glaze 91290_W (480 μm thick) must be interpreted with caution because this glaze exhibits severe degradation characterised by concentric pattern of alternating Sn- and Pb-rich rings (Fig. 4a and b), known as *Liesegang* rings [7], also found in other degraded architectural glazed ceramics at the Alhambra [28]. Bubbles, elongated rounded quartz – SiO_2 – bodies (Fig. 4c), and diopside – $CaMgSi_2O_6$ – precipitates (Fig. 4c–e) are observed. Chemical weathering is related with burial-induced transformation processes, wherein glazes are exposed to stagnant water. This environment promotes two concurrent weathering mechanisms: vitreous matrix dissolution and leaching of alkali elements. Low concentrations of Na_2O (0.37 wt.%) and K_2O (0.35 wt.%) suggest dealkalisation. Furthermore, weathering is marked by insoluble compounds precipitation, e.g., Ca/Pb-rich phosphates [31]. Notably, glaze 91290_W contains the highest P (8.86 wt.%) and Ca (CaO at 12.46 wt.%) concentrations of all studied white glazes (Table 2). Although some P could proceed from the soil, the high P concentration suggests that it could have been deliberately added to the glaze. Indeed, SEM-BSE images show tubular structures attributable to bone fragments (Fig. S1). Bone (fragments/ashes) have been used to opacify glass artifacts of diverse chronology, glazed tesserae and tableware ceramics and porcelain; however, its use is limited in glazed tiles [6,32,33]. Noteworthy, bone fragments were also detected in the ceramic body of Nasrid architectural ceramics in the Alhambra [28].

Chemical analysis of glaze 91290_W (Table 2) shows the average composition of three areas which include bubbles and rings (Fig. 4a and 4b). Some layers are low in Si, which accounts for the low SiO_2 content (Table 2). SEM analyses reveal that Si concentrates as quartz-rich bodies along *Liesegang* rings (Fig. 4a and c), whereas original unmelted quartz grains and

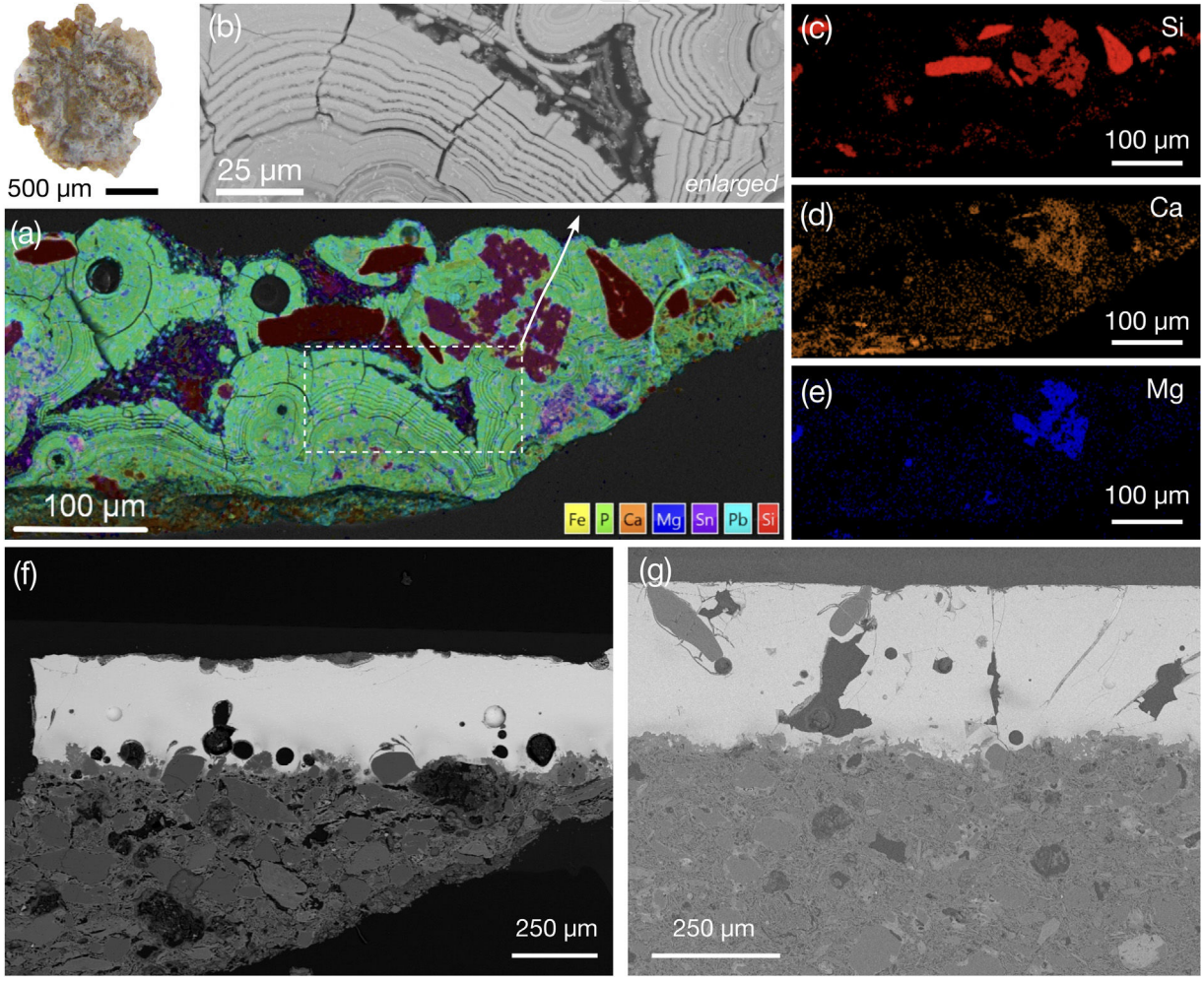

Fig. 4 – SEM-EDS images of white glazes. (a) X-ray map of glaze 91290_W showing *Liesegang* rings, see enlarged image in (b), and corresponding X-ray maps for Si (c), Ca (d) and Mg (e). (f) Glaze A085786/20_W with surface micropitting and (g) glaze 1294_W.

Please cite this article in press as: C. Cardell, et al., Archaeometric analysis of Nasrid glazed architectural ceramics from the Alhambra and Generalife Monument, Granada (Spain), Bol. Soc. Esp. Cerám. Vidr. (2025), https://doi.org/10.1016/j.bsecv.2025.100477

dendritic diopside remained unaltered (Fig. 4d and e; Table S4: sample 91290_W – spectrum 12 [34]). Note that diopside precipitation constrains the firing temperature to be above 900 °C [8].

Glazes 1382_W and 2264_W (14th century AD) exhibit great compositional variability, particularly in SnO_2 (16.24 wt.% and 4.03 wt.%), PbO (43.5 wt.% and 53.4 wt.%), Na_2O (1.51 wt.% and 3.10 wt.%), and K_2O (2.14 wt.% and 0.64 wt.%) (Table 2). This is surprising considering that both ceramics share typology and chronology, though proceed from different Nasrid palaces. Ceramic 1382 is from the Comares Palace, built by Yusuf I (1333–1354), whereas ceramic 2264 comes from the Lions Palace, constructed under Muhammad V (1362–1391). Muhammad V introduced design and technology innovations in the Alhambra ornamentation. He had a close alliance with the Christian king Pedro I of Castile. The emir sent craftsmen to the Palace of Pedro I, the Alcázar of Seville, built between 1356 and 1366. Consequently, the distinct composition of glazed ceramics from the Lions Palace is interpreted as intentional, rather than due to inadequate workmanship by Nasrid artisans.

Inlaid tiles, funerary stele and rooflight ceramic

White glazes of tiles A085786/20_W (280 μm thick) and 1294_W (320 μm thick) (Fig. 4f and g) exhibit similar SiO_2 contents, though differ in Al_2O_3, Na_2O, K_2O, and SnO_2 (Table 2). While both glazes are lead tin-opacified glazes [2], A085786/20_W is lower in alkalis (2.78 wt.%) and SnO_2 (6.85 wt.%) compared to 1294_W. Albite ($NaAlSi_3O_8$) subhedral aggregate crystals, some associated to acicular K–Pb feldspars, were found in A085786/20_W near the interface (Table S4, spectrum 136). Neither glaze contains large MgO amounts, as also found in the 14th century AD funerary stele glaze 1319_W (Fig. 2). This one exhibits the lowest SiO_2 (31.30 wt.%), K_2O (0.76 wt.%), Al_2O_3 (0.50 wt.%), and CaO (1.15 wt.%) contents among all analysed unweathered white glazes, though holds the highest PbO (52.25 wt.%) and SnO_2 (9.69 wt.%) concentrations (Table 2). This composition may serve as a ceramic typology fingerprint.

Glaze A085786/25_W (rooflight) composition precludes a straightforward classification according to Ref. [2] thereby distinguishing it from the other white glazes. This glaze (thickness ~180 μm) Exhibits 44.11 wt.% of PbO, the highest alkali content among the white glazes (2.88 wt.% Na_2O and 2.27 wt.% K_2O), the highest SiO_2 content (39.99 wt.%), and elevated CaO levels (2.67 wt.%). Conversely, its low PbO content suggest a specific recipe associated with this ceramic typology (Table 2).

Microstructure and morphological features

SEM observations reveal unmelted rounded quartz grains, and glaze–ceramic interfaces of varied thickness (~40 to 100 μm) in all white glazes (Fig. 4f and g). Although acicular K–Pb feldspar crystals are minute and discontinuous within some interfaces, their presence is widespread and, occasionally, accompanied by orthoclase ($KAlSi_3O_8$; glaze 1294_W, spectrum 140, Table S4). K and Al diffusion at interfaces suggest a single-firing process [2,7,35,36]. SEM microanalysis also revealed diopside in A085786/25_W glaze (spectra 48 and 49), and refractory unmelted aluminosilicate phases (Al_2SiO_5) in 1294_W (spectrum 186), a phase present in soils surrounding the city of Granada and sourced from the metamorphic rocks of Sierra Nevada mountain range.

Opacity in white glazes was achieved by varied cassiterite (SnO_2) amounts (Table 2), as in the other coloured studied glazes, also depending on ceramic typology. Likewise, crystal size and distribution within the glaze matrix differ (Fig. S2). Nanometric cassiterite crystals (500–800 nm), as found here, precipitate from the glaze ca. 900 °C; moreover, homogeneous distribution suggests the fritting method to elaborate the tin-glaze [37]. Islamic glazes – on pottery – from the Iberian Peninsula were rich in PbO and SiO_2, with contents varying according to coloured glazes. Quartz and feldspar inclusions, as here found in some white and coloured glazes, were likely used to enhance opacity, thus reducing costs derived from expensive tin oxide [37]. However, Ref. [38] states that the combined use of cassiterite and quartz for opacification, when one or the other would be enough, indicates that quartz was added to improve glaze viscosity. Considering the cassiterite amounts detected in all the studied glazes, enough to impart opacity, quartz/feldspars addition was not necessary, and may be related to glaze formulations used in these architectural ceramics [28].

White glazes recipes here analysed differ from those of the Mudejar Alcázar of Seville [17,39], containing less PbO and more SiO_2, although both comprise quartz and diopside. Also diverge from other al-Andalus and Mudejar white lead glazes, e.g., ceramic tableware of Paterna in Valencia, Spain [40], and those from the Monastery of Santa Clara-a-Velha in Coimbra (Portugal), which exhibit higher SnO_2 and lower PbO contents [5,41]. Al-Andalus glazes followed the single-firing technique typical of late Islamic glaze technology [40], as found here.

Blue glaze

Compositions differ according to ceramic typology (Table 2), all blue glazes being lead tin-opacified glazes [2]. PbO content ranges from 47.20 to 54.01 wt.% with increased Pb levels correlating to higher SnO_2 content. Alkalis are slightly higher in the 13th century AD glazes (3.94–4.05 wt.%) than the 14th century AD glazes (2.73–3.34 wt.%).

13th century AD blue glazes

Glazes 124965_BL (260 μm thick) and A085786/38_BL (180 μm thick) exhibit crazing, crawling and pitting surface weathering [42,43]. P associated with Ca and/or Pb and vanadium (V), is present in fissures and the glaze surface. Vanadium, indicative of burial conditions, was also found in weathered glazes of Nasrid architectural ceramics in the Alhambra [28,31]. P was not detected in the glaze matrices; however, apatite precipitates in sample A085786/38_BL suggests that P was part of the original glaze (Table 2). SEM reveals subhedral to dendritic diopside associated with wollastonite and albite which indicates firing temperatures between 900 and 1000 °C [7,8] and rapid crystallisation. Conversely, albite displays subhedral forms and dissolution patterns. Analogous albite crystals are abundant in the ceramic body, suggesting their incorporation into the glaze during the firing process. Notably, glaze

Please cite this article in press as: C. Cardell, et al., Archaeometric analysis of Nasrid glazed architectural ceramics from the Alhambra and Generalife Monument, Granada (Spain), Bol. Soc. Esp. Cerám. Vidr. (2025), https://doi.org/10.1016/j.bsecv.2025.100477

A085786/38_BL is rich in diopside and wollastonite, and subhedral and tubular apatite ($Ca_5(PO_4)_3(OH,F,Cl)$) crystals (Fig. S3). This observation agrees with other reports where apatite and Ca-rich silicates are often spatially related in Ca-saturated glazes [6]. Additionally, it suggests that apatite, likely as bone fragments/ashes, was intentionally added to the glaze either as opacifier or to improve glaze emulsification.

OM and EDS analyses reveal differences in the firing process of 124965_BL and A085786/38_BL compared to other coloured glazes, probably linked to the apatite addition. Unlike other glazes, the acicular K–Pb feldspar-rich interface appears as a continuous thin layer (<10 μm) of K-enriched glaze, along with a Si enrichment and Pb depletion. These features suggest a single-step firing process, though with a prominent physical interaction between the glaze and certain components of the ceramic body, notably albite and apatite crystals. These were likely detached from the ceramic body [35] and incorporated into the glaze due to their lower density relative to the lead glass, a process potentially enhanced by intense degassing of the ceramic body, also causing bubbles (~80 μm) and upward migration of immiscible Pb–Ca–P phase drops.

SEM investigation revealed that blue colour in glaze 124965_BL is due to Zn, Cu, Cr, Co, and Fe (Table 2), homogeneously dissolved in the glaze, rather than present as discrete precipitates [44]. In glaze A085786/38_BL, besides Cu and Zn dispersed in the glaze, Fe–Zn–Al precipitate (likely a franklinite-magnetite spinel, Table S4, spectrum 540) and Fe–Co-rich inclusions (Table S4, spectrum 532) were identified. Notably, Ni was not detected in these 13th century AD glazes. Noteworthy, in medieval glazes (tableware) from Valencia (Spain) there is an accepted evolution for Co-rich blue glazes based on chemical composition. Accordingly, the Co-Zn association is typical from the 12th and 13th century AD, while Ni is found in blue glazes from the 14th-15th century AD [45]. This supports the findings of this work and will validate the adscription of the blue glazes to the 13th century AD [30].

14th century AD blue glazes

Two blue tones from the funerary stele were analysed: 1319_LBL (light blue, 300 μm thick) and 1319_DBL (dark blue, 480 μm thick). Glazes contain abundant unmelted rounded quartz grains and have the lowest Ca content (CaO at 0.85–1.33 wt.%) among all blue glazes. They primary differ in detected blue chromophores. 1319_LBL contains lower amounts of Fe and Cu, while Co and Zn are not found in the matrix. Note that Co detection limit in EDS is 0.1 wt.%, and that lower Co amount can impart blue colour in enamels [6,28,41]. In glaze 1319_DBL, Fe, Co, Zn, and Cu are dissolved in the matrix. Additionally, Fe–Co–Zn-rich crystals are also recognised (Table S4). Both glazes exhibit surface pitting, with Ca-phosphates coating deposits. In 1319_LBL, surface is enriched in Co, Fe, and notably Cr, suggesting an overglaze decoration, while traces of Cu are dispersed throughout the glaze [6,17,44]. As discussed later, Cu is the key chromophore in green-turquoise glazes, aligning with the tendency of this light blue glaze to exhibit a turquoise hue.

Glaze 1294_BL (250 μm thick) is comparable to glaze 124965_BL, as both exhibit crazing, and differ from A085786/38_BL, less affected by cracking. Surface of 1294_BL is unaltered. The glaze–ceramic interface is well-defined though enriched in acicular K–Pb feldspars, suggesting a single firing [8]. Skeletal wollastonite (spectrum 137, Table S4) aggregates (>200 μm) are present in the glaze. Blue colour is due to Co, Cu, Fe, and Zn dissolved in the matrix (Table 2). No Fe–Co–Zn-rich inclusions are observed, though scarce diopside crystals are detected.

Weathered *sebka* glaze 132766_BL (150 μm thick) exhibits cracking and bubbles with walls coated with neoformed SiO_2-rich Al–Ca minerals (Fig. 5a and b). Large bubbles suggest a relatively low-viscosity glass phase promoting evacuation of gas-filled bubbles formed by the intense degassing of the ceramic body [11]. Well-defined glaze–ceramic interface is K-enriched (Fig. 5e) and Si depleted, likewise A085786/38_BL, which according to Ref. [8] indicates a once-firing process. Weathering progressed along the interface, leading to Pb depletion and P enrichment (Fig. 5c and d) that does not correspond with the K-enriched layer (Fig. 5e). K interface enrichment and thin K–Pb acicular feldspars (Fig. 5b) might suggest the use of a slip where the glaze mixture was applied over the already-fired ceramic body. Alternatively, as discussed above regarding the albite and Pb–Ca–P immiscible phase drops, likely indicate a physical interaction with the ceramic body enhanced by the low viscosity of the lead glass.

Furthermore, curved apatite crystals (Fig. 5d) are in the ceramic body, suggesting that some were incorporated into the glaze during firing. This hypothesis is supported by the rounded, immiscible Pb–Ca–P glaze phases located beneath the interface and within the glaze, frequently associated with bubbles (Fig. 5d). In Albanian 12th–13th century AD glazed ceramics P was added as both a flux and as modifying agent in green-ocean glazes [34]. Authors reported a crystallisation sequence involving apatite and related phosphate and arsenate minerals. Additional studies suggest that P may enhance the blue colour in Cu-based enamels [44]. Blue colour results from Co, Cu, Zn, and Fe dissolved within the glaze (Table 2). Notably, Ni – characteristic of 14th–15th century AD Valencian glazes [45] – was not detected in any of the studied 14th century AD blue glazes. Therefore, results suggest a chronological reassessment of these ceramics.

Green-turquoise glaze

Chemical composition

Glaze composition varies according to ceramic typology (Table 1 and Fig. 2) and location in the monument. However, all can be classified as lead tin-opacified glazes [2], although PbO is lower – for this classification – in 124965_GT, 121708_GT, and 2264_GT (Table 2). Green-turquoise glazes exhibit the highest variability in composition and some of the lowest PbO contents of all studied glazes (except for black glazes). The highest SnO_2 quantity is found in the *sebka* glaze (132766_GT, 8.22 wt.%), followed by the 13th century AD tile glazes (6.10 and 6.97 wt.%). Notably, SnO_2 in glaze 2264_GT is quite low (0.47 wt.%). SnO_2 levels are higher than in other green-turquoise glazes from the Alhambra [28]. Alkali elements are below 5 wt.%, with Na more abundant than K (Table 2). This quantity is lower than in analogous Alham-

Please cite this article in press as: C. Cardell, et al., Archaeometric analysis of Nasrid glazed architectural ceramics from the Alhambra and Generalife Monument, Granada (Spain), Bol. Soc. Esp. Cerám. Vidr. (2025), https://doi.org/10.1016/j.bsecv.2025.100477

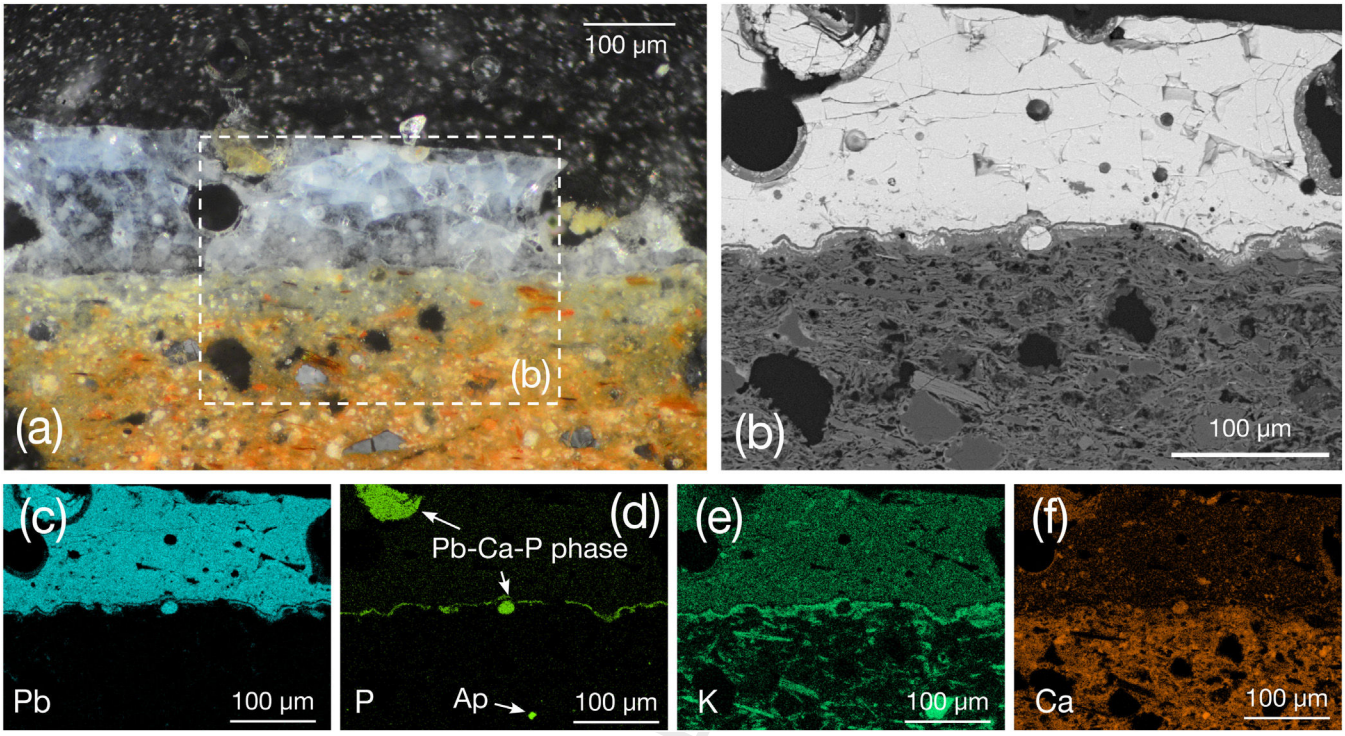

Fig. 5 – Blue glaze *sebka* ceramic type (132766_BL). (a) Cross-polarised OM image highlighting the area were the BSE (b) and X-ray map were acquired for (c) Pb, (d) P, (e) K and (f) Ca.

bra glazes [28], but higher than in some Mudejar architectural ceramics [17,39].

Green-turquoise colour results from Cu (expresses as CuO, Table 2) dissolved in the matrix under oxidising conditions. The highest CuO content (3.50 wt.%) is found in the *sebka* glaze (132766_GT). Contrary to other Alhambra turquoise glazes, no Co is found in these glazes, though Fe is detected. Copper is present in oxidising environments as Cu^{2+} or Cu^{+}, producing colours from bottle green to turquoise [6,44]. Hue depends on the Pb and alkali glaze contents. Green-turquoise colours occur in glazes with PbO <45 wt.%, as found here (Table 2), except for A085786/19_GT (47.31 wt.%) and 132766_GT (50.87 wt.%). These glazes are not alkali-rich, unlike previously studied turquoise glazes [28].

Microstructure and morphological features

SEM investigation (Fig. 6) of green-turquoise glazes reveals variations in microstructure, composition, and firing processes. Glazes 121708_GT (90 µm thick) and A085786/19_GT (320 µm thick) exhibit pitting, bubbles, and fissures (Fig. 6a and b). Aggregated cassiterite crystals are found in the glazes, and wollastonite is abundant. The glaze–ceramic interface contains K-rich acicular crystals, suggesting a single-firing process. Glaze 124965_GT (210 µm thick) exhibits a homogeneous glaze without evidence of weathering. The interface is clean indicating double-firing process.

The *sebka* glaze 132766_GT (220 µm thick) exhibits surface pitting, and early-stage banding where P was detected (Fig. 6c). Glaze 2264_GT (220 µm thick) displays cracked and pitted surface with abundant medium-sized bubbles (Fig. 6d). Aggregated cassiterite and wollastonite precipitates are abundant. Wollastonite contains Cr (up to 0.8 wt.% Cr_2O_3, spectrum 45, Table S4), which probably contribute to the green colour. Notably, the composition and microstructure of the dark green-turquoise 2264_GT glaze differs substantially from the others.

Black glaze

All black glazes originate from tiling mosaic panels (Tables 1 and 2) and contain no SnO_2.

13th century AD glazes

Glaze 91288_BK is unique, as it is not in contact with the ceramic body. This ceramic has never undergone intervention. SEM-BSE study revealed that the black decoration was applied over a Ca-rich layer (~150 µm thick) consisting of two parts: 91288_BK_m1 and 91288_BK_m2 (Fig. 7a). The lower part (91288_BK_m1) shows dissolution processes and precipitation that results in elongated crystals exceeding 50 µm in length, near the interface with the ceramic body, made solely of Ca, likely in the form of lime – $Ca(OH)_2$ – or calcite – $CaCO_3$ –. EDS analyses show composition in wt.% oxides; thus, Ca is shown as CaO, though Ca may be part of other minerals, e.g., calcite or apatite.

The upper part (91288_BK_m2) contains CaO (72.12 wt.%) and PbO (21.19 wt.%, Table 2). High Pb levels at the top of 91288_BK_m2 are associated with a short (ca. 30 µm) diffusion process between the glaze (bright colour in surface in Fig. 7a)

Please cite this article in press as: C. Cardell, et al., Archaeometric analysis of Nasrid glazed architectural ceramics from the Alhambra and Generalife Monument, Granada (Spain), Bol. Soc. Esp. Cerám. Vidr. (2025), https://doi.org/10.1016/j.bsecv.2025.100477

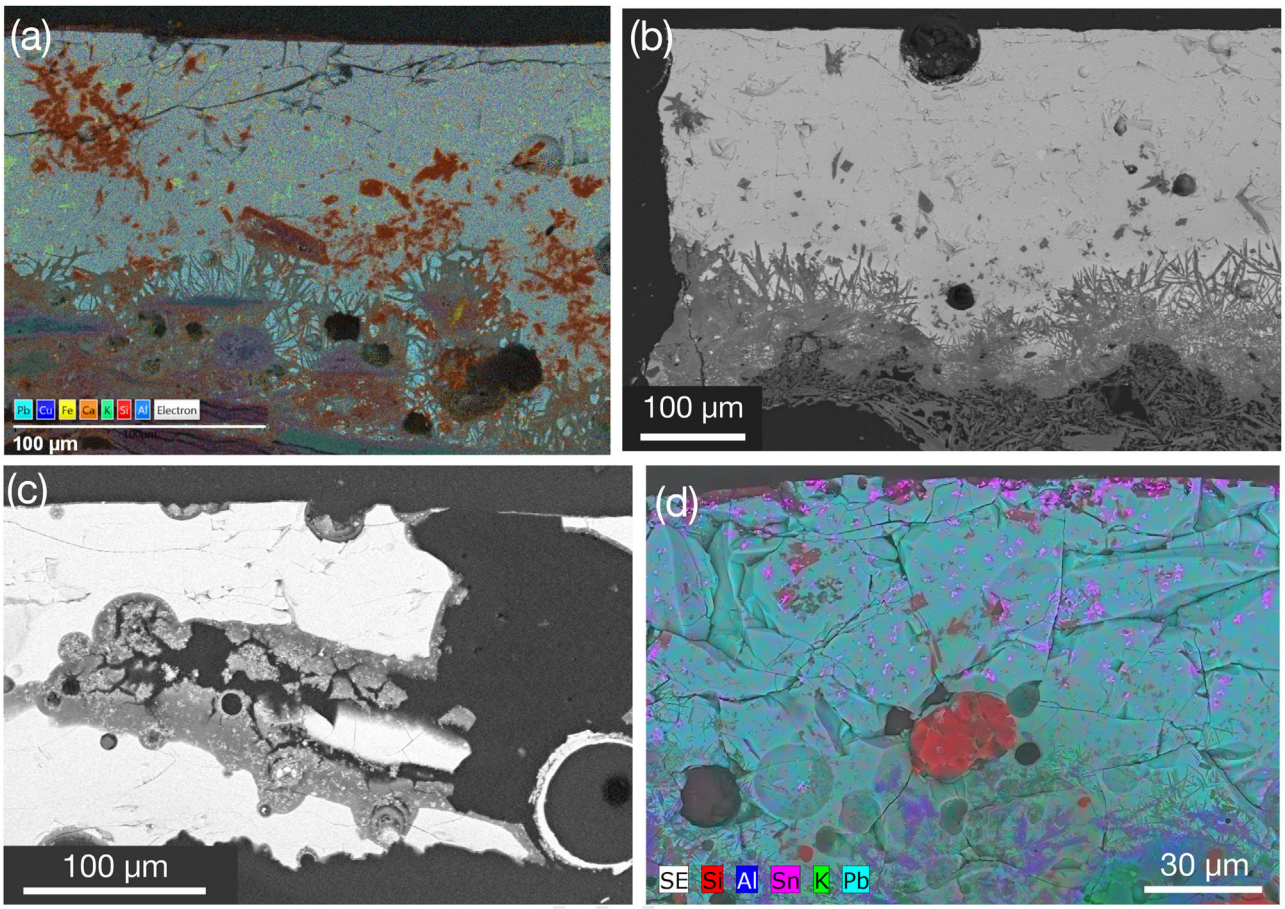

Fig. 6 – Green-turquoise glaze. (a) X-ray map of 121708_GT showing wollastonite precipitates in brown-red. (b) BSE image of A08578619_GT exhibiting K–Pb feldspar crystals in the interface, (c) BSE image of 132766_GT displaying intense weathering, (d) X-ray map of 2264_GT showing rounded quartz (red), cassiterite (pink) and wollastonite (bluish) precipitates.

and the Ca-rich substrate due to weathering. Glaze 91288_BK_g is exceptionally thin (ca. 25 µm) and exhibits extensive weathering. This results in chemically alternating skinny layers that caused variations in Si–Pb–P parallel to the surface (Fig. 7a). Dark colour is due to Mn (MnO up to 15.01 wt.%, Table 2) in the outermost layer of 91288_BK_g. This layer has the lowest SiO_2 content (7.14 wt.%) and the highest PbO content (65.24 wt.%) among all studied glazes. Vanadium related to burial processes [31] was also detected.

The alternating Si–Pb–P layers are interpreted as corrosion features, termed lamellae [46]. Lamellae form due to ion exchange between the glaze and an aqueous fluid, leading to Pb and alkali metals diffusion from the glaze into the aqueous solution [46]. This process increases the pH at the glaze-fluid interface, liberating SiO_2 into the aqueous phase as silicic acid while hydrous components incorporate into the glaze. Probably, weathering of glaze 91288_BK is related to post-depositional transformations in a wet environment after burial and aligns with the high P and Pb concentration [31]. Precipitation of fine-grained secondary phases due to the post-burial process cannot be excluded. Indeed, Ca, Fe, and Al associated with P might correspond to tiny secondary minerals previously identified [31,47,48], e.g. vivianite ($Fe_3(PO_4)_2{\cdot}8(H_2O)$), mitridatite ($Ca_2Fe_3(PO_4)_3O_2{\cdot}3(H_2O)$), crandallite ($CaAl_3(PO_4)_2(OH)_5{\cdot}(H_2O)$) and pyromorphite ($Pb_5(PO_4)_3Cl$). However, Cl could not be identified (2.62 keV in EDS spectra) because high Pb amount that has several lower-intensity M-lines that overlap in this region. Vanadium suggests the occurrence of vanadinite ($Pb_5(VO_4)_3Cl$).

14th century AD glazes

The two studied glazes are significantly different. Glaze 2264_BK is thick (480 µm) and exhibits scarce bubbles but extensive crazing (Fig. 7b and 7c). Colour is due to Mn (MnO 4.74 wt.%) and iron expressed as Fe_2O_3 (4.08 wt.%, Table 2). Its glaze–ceramic interface is thick and diffuse (~100 µm), characterised by Mn depletion, Al and K enrichment and acicular crystals (Fig. 7c) suggesting a single-firing process [7,35]. Crystal's composition corresponds to K-feldspar and diopside, unlike acicular minerals in the interface of other studied glazes composed of K–Pb feldspar.

Surprisingly, OM investigation of sample 1382_BK reveals that is not a glaze (Fig. 7d). EDS analyses are compatible with quartz, muscovite, and biotite ($K(Mg,Fe)_3AlSi_3O_{10}(OH,F)_2$) crystals, suggesting a fine-grained mica-schist or slate are present, both abundant in the nearby Sierra Nevada Mountain range

Please cite this article in press as: C. Cardell, et al., Archaeometric analysis of Nasrid glazed architectural ceramics from the Alhambra and Generalife Monument, Granada (Spain), Bol. Soc. Esp. Cerám. Vidr. (2025), https://doi.org/10.1016/j.bsecv.2025.100477

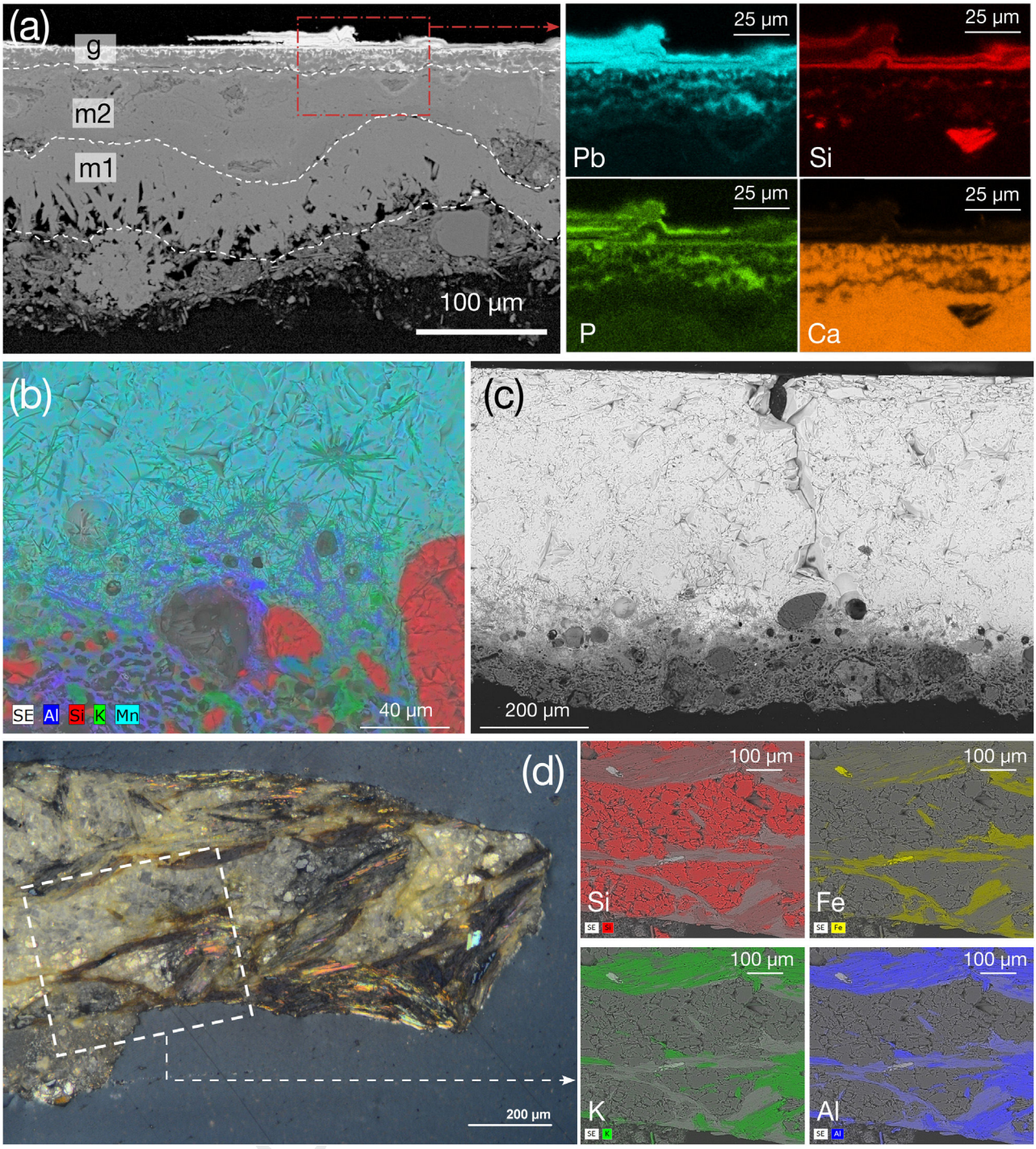

Fig. 7 – Textures seen in black coloured samples (a) BSE image of 91288_BK showing large prismatic crystals in the lower layer (m1) perpendicular to the interface. Another lime-rich layer (m2) between layer m1 and the glaze (g). The area highlighted in dashed red lines correspond to the X-ray maps for Pb, Si, P, Ca on the right, (b) X-ray map of 2264_BK displaying K–Pb feldspar at the interface, (c) BSE image of 2264_BK showed in (b) illustrating a well-developed interface, (d) cross-polarised OM image of the black coloured ceramic 1382_BK exhibiting biotite, mica flakes and quartz aggregates (X-ray maps are showed at the right and highlighted in (d)).

(Granada). Black colour is likely due to the colour of Fe-bearing biotite and/or the presence of graphite. This finding demonstrates that Nasrid tile-makers possessed the technical skills to cut and polish these rock fragments to a thickness of ~300 µm. The method by which these fragments were integrated into the ceramic body remains uncertain, as they could not have been fired in the kiln simultaneously with the raw clay. Considering the firing temperatures attained by ceramic bodies of Nasrid architectural ceramics, ca. 950 °C [28], significant mineralogical and textural changes would have occurred

Please cite this article in press as: C. Cardell, et al., Archaeometric analysis of Nasrid glazed architectural ceramics from the Alhambra and Generalife Monument, Granada (Spain), Bol. Soc. Esp. Cerám. Vidr. (2025), https://doi.org/10.1016/j.bsecv.2025.100477

in the metamorphic rock (not observed in the studied sample), i.e., decomposition of micas, possible oxidation of graphite or iron, and potential vitrification of feldspars. These transformations could render the rock more brittle and alter its colour and texture. Therefore, the petrographic study suggests that the ceramic body was fired separately to the decoration. Possibly the rock fragments were shaped, polished, and applied to the ceramic surface post-firing, using mechanical embedding technique (inlaid into pre-prepared recesses on the surface) or adhesives. Like this, tile-makers would have preserved the metamorphic rock appearance while ensuring its integration into the mosaic. Indeed, the substrate of sample 1382_BK, directly beneath the rock fragments, is enriched in carbonates. This suggests that the Nasrid artisans may have used a mortar to adhere the fragments to the ceramic body of the tiling mosaic panel.

Honey glaze

The 14th century AD studied honey glazes were taken from the sampled tiling mosaic panels decorated in white and black (Fig. 2). Although honey glazes are compositionally similar, each glaze shows peculiarities related to weathering and microstructure.

Glaze 1382_H (thickness ~150 μm) shows bubbles (>50 μm), crazing and weathering (Fig. 8a). Phosphorus was detected in the glaze matrix. Large bubbles suggest degassing from the ceramic body [11]. Wollastonite prismatic crystals are frequent, alike similar coloured glaze in Ref. [17], and evenly distributed throughout the glaze, while SnO_2 precipitates are less frequent (Fig. 8a). It is known that wollastonite may incorporate impurities such as Fe, K, Mn, Mg, or Na. However, here Cr was detected (0.64 wt.% Cr_2O_3, spectrum 12, Table S4), resembling those found in the Cr-bearing wollastonite from the green-turquoise glazes.

It could be argued that Cr comes from pigment chrome yellow, whose natural form is the mineral crocoite ($PbCrO_4$). It was first used in 1818, and employed in ceramics, varnishes, and high-temperature paints [49,50]. If chrome yellow was used in glaze 1382_H, it will indicate that this piece was produced and incorporated into the mosaic panel during the 19th century AD onward, though no documentation exists. Honey colour probably results from Fe^{3+} (3.15 wt.% Fe_2O_3, Table 2) fired in an oxidising atmosphere. Another particularity of this glaze is the association of Fe with Ti (expressed as TiO_2 at 0.22 wt.%, Table 2) similarly as in the black glaze of the same mosaic panel (1382_BK). Glaze–ceramic interface is sharp, with no K–Pb feldspars, suggesting double-firing and supporting the hypothesis that this piece was involved in a restoration.

Two honey glaze samples from the mosaic panel 2264 (Fig. 2), exhibiting distinct hue, were studied. Glaze 2264_H2 is ~200 μm thick, contains large bubbles (~90 μm) and elongated euhedral Cr-bearing wollastonite crystals (Fig. 8b and c, indi-

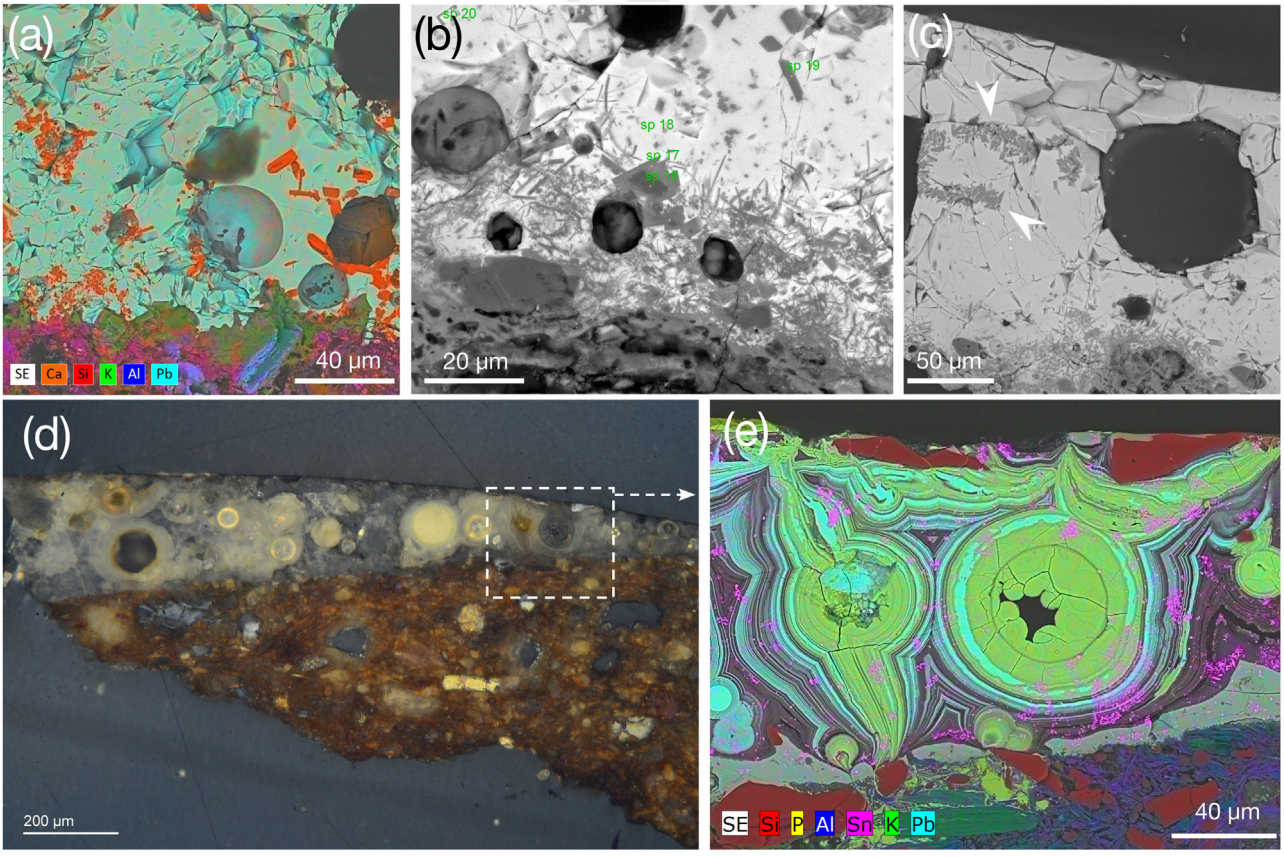

Fig. 8 – Honey glazes. (a) X-ray map of 1382_H showing wollastonite prismatic crystals (orange), (b and c) BSE image of 2264_H2 displaying large bubbles and wollastonite crystals (white arrows), (d) cross-polarised OM image of 2264_H1 highlighting the area of the X-ray map showed in (e) with *Liesegang* rings, cassiterite (pink) and quartz-rich bodies (red).

Please cite this article in press as: C. Cardell, et al., Archaeometric analysis of Nasrid glazed architectural ceramics from the Alhambra and Generalife Monument, Granada (Spain), Bol. Soc. Esp. Cerám. Vidr. (2025), https://doi.org/10.1016/j.bsecv.2025.100477

cated by arrows), as in glaze 1382_H. However, unlike 1382_H, barium (Ba) together with scarce Fe was detected in 2264_H2, both dissolved in the glaze and in Ca–K–feldspar crystals (in Fig. 8b; spectrum 629, Table S4). These features are unique to glaze 2264_H2 and, along with the Cr-bearing wollastonite in the green-turquoise glaze of the same piece (2264_GT, spectrum 45, Table S4), suggest that both glazes may have been produced in the 19th or 20th century AD. Nonetheless, Ba may also derive from burial environments [31,49]. The thick interface of 2264_H2, rich in K–Pb feldspars, suggests a once-firing process, unlike sample 1382_H.

Glaze 2264_H1 (thickness ~80–240 μm, Fig. 8d) exhibits extensive weathering, showing *Liesegang* rings made of alternating Sn and Pb (Fig. 8e). Glaze shows agglomerated dendritic SnO_2 crystals – that do not support the use of glaze fritting technique [37]– and elongated quartz-rich bodies near surface (Fig. 8e). Additionally, Ca/Pb-rich phosphates were identified. P correlates to Ca, attesting for Ca-phosphate minerals, locate in microcracks and reach the glaze–ceramic interface.

Conclusions

Analysed glazes show chemical and microstructural variability related with colour and ceramic typology; however, all correspond to lead tin-opacified glazes. Microstructural features, e.g., glaze–ceramic interfaces, and acicular K–Pb feldspars occurrence, indicate that single-firing processes were dominant. Frequent bubbles, diffusive elemental profiles, and immiscible crystalline phases support this conclusion. Glazes were elaborated at low temperature (~900 °C) in an oxidising atmosphere. Often, quartz inclusions are present in glazes; rather than considering a process of glaze double opacity, the high cassiterite amounts of glazes suggest that quartz was added to improve glaze viscosity. Phosphorus associated with burial weathering was identified. Furthermore, in some white and blue glazes, P is related to the use of bone fragments or ashes. This addition was likely intended to enhance glaze emulsification rather than to serve as an opacifier, given the cassiterite contents. The most significant inferences from this study are shown below.

While some white glazes are well preserved, others exhibited severe weathering characterised by *Liesegang* rings, alkali depletion, and P-rich corrosion phases. Such weathering complicates chemical glaze analysis and highlights the importance of burial environments in modifying glaze composition. Moreover, differences between Nasrid white glazes with less SiO_2 and more PbO than those from Mudejar contexts (e.g., Real Alcázar of Seville) suggest regional and chronological distinctions in glaze technology.

Blue glazes are mainly coloured by dissolved Co, Cu, Zn, and Fe in the glaze. Notably, Ni – commonly present in 14th–15th century AD Valencian glazes – is absent, raising questions about the chronological attribution, based on stylistics studies, of certain analysed ceramics to the 14th century AD. The greenish hue of some blue glazes is associated with Cr-bearing wollastonite, possibly indicating deliberate compositional control. These findings (and others discussed in the text) suggest diverse recipes and sources for the chromophores, and occasionally, technical innovations specific to Muhammad V's court. Regarding the green-turquoise glazes, they exhibited a more complex chromophore system, with Cu as the principal chromophore and Cr-bearing wollastonite contributing to colour modulation.

Black glazes are distinguished by their lower PbO contents. Colour is due to Fe and Mn oxides dissolved in the glaze. A black decoration was identified as a polished micas-chist rock intentionally cut and set into the tile mosaic panel. Concerning the honey glazes, some may reveal interventions, considering the presence of Ba-bearing K-feldspars and Cr-bearing wollastonite. This is a hypothesis in line with historical records of restoration.

Finally, a more extensive study of compositional anomalies in glazes (e.g., presence/absence of Ba, Ni, Cr, V, etc.) would be required to assess issues related to chronology, late post-deposition weathering, or later ceramic interventions. These results also illustrate the power of combining chemical, microstructural, and contextual analysis, with historians and archaeologists' knowledge to understand both ancient technological choices and modern conservation interventions in Islamic architectural ceramics.

Funding

Funding was provided by Research Project PID2023-146405OB-100 of Ministry of Science Innovation and Universities (MICIU/AEI/10.13.039/501100011033,x), Research Group RNM-179 of Junta de Andalucía (Spain), and Research Excellence Unit "Science in the Alhambra" (UCE-PP2018-01) of University of Granada (Spain). M. Urosevic acknowledges funding through the Spanish PTA program (PTA2022-021516-I).

Acknowledgments

We thank the Alhambra and Generalife Council, and to Silvia Pérez and Eva Moreno from the Alhambra Museum's private storage, as well to María Elena Díez Jorge for providing critical insights into these ceramics. We acknowledge the constructive comments of the two anonymous reviewers, which have significantly contributed to improving the clarity and overall quality of the manuscript.

Appendix A. Supplementary data

Supplementary data associated with this article can be found in the online version available at https://doi.org/10.1016/j.bsecv.2025.100477.

REFERENCES

[1] G.E. De Benedetto, P. Acquafredda, M. Masieri, G. Quarta, L. Sabbatini, P.G. Zambonin, M. Tite, M. Walton, Investigation on roman lead glaze from Canosa: results of chemical analyses, Archaeometry 46 (2004) 615–624, http://dx.doi.org/10.1111/j.1475-4754.2004.00177.x.
[2] M.S. Tite, I. Freestone, R. Mason, J. Molera, M. Vendrell-Saz, N. Wood, Lead glazes in antiquity – methods of production

and reasons for use, Archaeometry 40 (1998) 241–260, http://dx.doi.org/10.1111/j.1475-4754.1998.tb00836.x.
[3] M. Tite, O. Watson, T. Pradell, M. Matin, G. Molina, K. Domoney, A. Bouquillon, Revisiting the beginnings of tin-opacified Islamic glazes, J. Archaeol. Sci. 57 (2015) 80–91, http://dx.doi.org/10.1016/j.jas.2015.02.005.
[4] P. Holakooei, S. Soldi, J.-F. De Lapérouse, F. Carò, Glaze composition of the Iron Age glazed ceramics from Nimrud, Hasanlu and Borsippa preserved at The Metropolitan Museum of Art, J. Archaeol. Sci. Rep. 16 (2017) 224–232, http://dx.doi.org/10.1016/j.jasrep.2017.09.031.
[5] S. Coentro, L.C. Alves, C. Relvas, T. Ferreira, J. Mirão, J. Molera, T. Pradell, R.A.A. Trindade, R.C. Da Silva, V.S.F. Muralha, The glaze technology of Hispano-Moresque ceramic tiles: a comparison between Portuguese and Spanish collections, Archaeometry 59 (2017) 667–684, http://dx.doi.org/10.1111/arcm.12280.
[6] P. Colomban, Colouring agents for glass, glaze and enamel: tracing innovation and exchange routes, in: P. Vandenabeele, H. Edwards (Eds.), Raman Spectroscopy in Archaeology and Art History, vol. 2, Royal Society of Chemistry, London, 2019.
[7] T. Pradell, J. Molera, Ceramic technology. How to characterise ceramic glazes, Archaeol. Anthropol. Sci. 12 (2020) 189, http://dx.doi.org/10.1007/s12520-020-01136-9.
[8] J. Molera, J.C. Carvajal López, G. Molina, T. Pradell, Glazes, colourants and decorations in early Islamic glazed ceramics from the Vega of Granada (9th to 12th centuries CE), J. Archaeol. Sci. Rep. 21 (2018) 1141–1151, http://dx.doi.org/10.1016/j.jasrep.2017.05.017.
[9] J. Molera, V. Martínez Ferreras, A. Fusaro, J.M. Gurt Esparraguera, M. Gaudenzi, S.R. Pidaev, T. Pradell, Islamic glazed wares from ancient Termez (southern Uzbekistan). Raw materials and techniques, J. Archaeol. Sci. Rep. 29 (2020), http://dx.doi.org/10.1016/j.jasrep.2019.102169, 102169.
[10] M. Maggetti, SEM study of black, blue, violet and yellow inglaze colours of the oldest Swiss tin-opacified stove tiles (c.1450–c.1512, canton Bern), Archaeometry 63 (2021) 721–737, http://dx.doi.org/10.1111/arcm.12638.
[11] F. Agua, Á. Sánchez-Cabezudo, A. Pérez de Tudela, M.Á. Villegas, M. García-Heras, Archaeometric case-study of tiles of different dates from the Royal Monastery of San Lorenzo de El Escorial (Spain), Bol. Soc. Esp. Ceram. Vidr. 61 (2022) 84–97, http://dx.doi.org/10.1016/j.bsecv.2020.09.001.
[12] M. Tite, T. Pradell, A. Shortland, Discovery, production and use of tin-based opacifiers in glasses, enamels and glazes from the Late Iron Age onwards: a reassessment, Archaeometry 50 (2008) 67–84, http://dx.doi.org/10.1111/j.1475-4754.2007.00339.x.
[13] L.F. Vieira Ferreira, T.M. Casimiro, C. Boavida, M.F. Costa Pereira, I. Ferreira Machado, An archaeometric study of lead-glazed medieval ceramics (13th–14th century) from Santarém, Portugal, Heritage 7 (2024) 2217–2238, http://dx.doi.org/10.3390/heritage7050105.
[14] I. Ortega-Feliu, B. Gómez-Tubío, Y. Cáceres, M.Á. Respaldiza, Characterization of glaze ceramics from the archaeological site of La Alcazaba, Almería (Spain), Microchem. J. 138 (2018) 72–81, http://dx.doi.org/10.1016/j.microc.2017.12.022.
[15] M. Matin, M. Tite, O. Watson, On the origins of tin-opacified ceramic glazes: new evidence from early Islamic Egypt, the Levant, Mesopotamia, Iran, and Central Asia, J. Archaeol. Sci. 97 (2018) 42–66, http://dx.doi.org/10.1016/j.jas.2018.06.011.
[16] J. Mimoso, A. Pleguezuelo, M. Antunes, D. Costa, S. Morais Pereira, A. Silva, A Technical Overview of 16th Century Majolica Tiles From Palácio e Quinta da Bacalhôa in Portugal, LNEC, 2021, Available from: http://repositorio.lnec.pt:8080/xmlui/handle/123456789/1014630.
[17] J.L. Pérez-Rodríguez, M.D. Robador, J. Castaing, L. De Viguerie, M.A. Garrote, A. Pleguezuelo, Caracterización arqueométrica (físico-química y microestructural) de azulejos en el palacio mudéjar del Real Alcázar de Sevilla mediante métodos químicos cuantitativos no invasivos, Bol. Soc. Esp. Ceram. Vidr. 60 (2021) 211–228, http://dx.doi.org/10.1016/j.bsecv.2020.03.001.
[18] E. Salinas, J. De Juan, J.M. Piñero, M.T. Casal, N. Schibille, T. Pradell, From glass to glaze in al-Andalus: local invention and technological transfer, Eur. J. Archaeol. 25 (2022) 22–41, http://dx.doi.org/10.1017/eaa.2021.23.
[19] T. Pradell, J. Molera, A.D. Smith, M.S. Tite, Early islamic lustre from Egypt, Syria and Iran (10th to 13th century AD), J. Archaeol. Sci. 35 (2008) 2649–2662, http://dx.doi.org/10.1016/j.jas.2008.05.011.
[20] M.M. Raith, N. Abdali, P.A. Yule, Petrochemical attributes of glazed architectural elements from Middle-Elamite to Achaemenid excavation sites in Iran, Archaeol. Anthropol. Sci. 14 (2022) 182, http://dx.doi.org/10.1007/s12520-022-01648-6.
[21] M.E. Díez Jorge, I.B. Maturana, N.J. Díaz, The Alhambra: transformation and change through architectural ceramics, Arts 7 (2018) 79, http://dx.doi.org/10.3390/arts7040079.
[22] D. Dias Martins, The Alhambra museum: history, conservation and management of its tile and tiling mosaic collections, GEC 25 (2024) 106–116, http://dx.doi.org/10.37558/gec.v25i1.1259.
[23] M.E. Díez Jorge, Una ciudad de cerámica: alicatados, azulejos y otros barros en la Alhambra, Patronato de la Alhambra y Generalife, 2022, Available from: https://digibug.ugr.es/handle/10481/93954. (Accessed 6 June 2025).
[24] F. González García, M. González Rodríguez, M.C. González Vilches, A. Vallejo Triano, Estudio arqueométrico de algunas cerámicas medievales de Madinat Al-Zahra (Córdoba), (1992), Bol. Soc. Esp. Ceram. Vidr. 31 (1992) 491–498.
[25] P. Marinetto Sánchez, Elementos de columnas nazaríes en cerámica vidriada, in: Ante el nuevo milenio. Raíces culturales, proyección y actualidad del arte español: XIII Congreso Nacional de Historia del Arte, vol. 1, Universidad de Granada, Granada, del 31 de octubre al 3 de noviembre de 2000, 2000, pp. 167–178, ISBN 84-8444-193-8. Available from: https://dialnet.unirioja.es/servlet/articulo?codigo=3231979. (Accessed 6 June 2025).
[26] P. Marinetto Sánchez, Cerámica arquitectónica nazarí. Algunos ejemplos de piezas pintadas, in: Ante el nuevo milenio. Raíces culturales, proyección y actualidad del arte español: XIII Congreso Nacional de Historia del Arte, vol. 1, Universidad de Granada, Granada, del 31 de octubre al 3 de noviembre de 2000, 2000, pp. 153–167, ISBN 84-8444-193-8. Available from: https://dialnet.unirioja.es/servlet/articulo?codigo=3231977. (Accessed 6 June 2025).
[27] G. Degeorge, Y. Porter, L'art de la céramique dans l'architecture musulmane, Flammarion, Paris, 2001, ISBN 208010568X.
[28] C. Cardell Fernández, I. Guerra Tschuschke, Estudio arqueométrico de cerámicas arquitectónicas vidriadas decoradas de los fondos del Museo de la Alhambra, in: Hecha de barro y vestida de color: Cerámica arquitectónica en la Alhambra, vol. 1, Patronato de La Alhambra y Generalife (Estudios), 2022, pp. 235–269, ISBN 9788417518165.
[29] M. Melgosa, F.J. Collado-Montero, E. Fernández, V.J. Medina, Estudio colorimétrico de los azulejos del Patio de las Doncellas del Real Alcázar de Sevilla (España), Bol. Soc. Esp. Ceram. Vidr. 54 (2015) 109–118, http://dx.doi.org/10.1016/j.bsecv.2015.03.002.
[30] M. Busto Zapico, A. García Porras, Ceramic production and social change in the south east of the Iberian Peninsula between the islamic and christian periods: the case of

Please cite this article in press as: C. Cardell, et al., Archaeometric analysis of Nasrid glazed architectural ceramics from the Alhambra and Generalife Monument, Granada (Spain), Bol. Soc. Esp. Cerám. Vidr. (2025), https://doi.org/10.1016/j.bsecv.2025.100477

Granada, Int. J. Histor. Archaeol. 26 (2022) 715–739, http://dx.doi.org/10.1007/s10761-021-00619-2.
[31] L. Maritan, Ceramic abandonment. How to recognise post-depositional transformations, Archaeol. Anthropol. Sci. 12 (2020) 199, http://dx.doi.org/10.1007/s12520-020-01141-y.
[32] M. Beltrame, CALIPH: Comprehensive Archaeological and Laboratory Investigation of Islamic Pottery in Portuguese History, Universidade de Évora, Portugal, 2022.
[33] H. Wu, H. Li, Y. Wang, P. He, Z. Li, Q. Ma, Was bone used in the glaze of the ancient Qiong kilns for the production of tang dynasty opaque glaze celadon? J. Eur. Ceram. Soc. 45 (2025), http://dx.doi.org/10.1016/j.jeurceramsoc.2024.117017, 117017.
[34] M.G. Perna, F. Falcone, C. Casolino, E. Metalla, G. Rosatelli, S. Antonelli, F. Stoppa, Analysing the glaze of a medieval ceramic fragment from the Durres Amphitheater in Albania, Herit. Sci. 12 (2024) 82, http://dx.doi.org/10.1186/s40494-024-01175-8.
[35] J. Molera, T. Pradell, N. Salvadó, M. Vendrell-Saz, Interactions between clay bodies and lead glazes, J. Am. Ceram. Soc. 84 (2001) 1120–1128, http://dx.doi.org/10.1111/j.1151-2916.2001.tb00799.x.
[36] M.S. Madrid Fernandez, J. Buxeda Garrigós, Exploring the Technique of Glazing used by the Potters of Barcelona, 2021, http://dx.doi.org/10.5281/zenodo.5598243.
[37] J. Pérez-Arantegui, P. Marzo, Characterization of Islamic ceramic production techniques in northeast Iberian Peninsula: the case of medieval Albarracin (Spain), Appl. Sci. 11 (2021) 7212, http://dx.doi.org/10.3390/app11167212.
[38] E. Salinas, T. Pradell, The secret is quartz: technology of production of an eleventh-twelfth century western Mediterranean polychrome glazed ware, Archaeol. Anthropol. Sci. 16 (2024), http://dx.doi.org/10.1007/s12520-024-02040-2.
[39] I. Garofano, M.D. Robador, J.L. Perez-Rodriguez, J. Castaing, C. Pacheco, A. Duran, Ceramics from the Alcazar Palace in Seville (Spain) dated between the 11th and 15th centuries: compositions, technological features and degradation processes, J. Eur. Ceram. Soc. 35 (2015) 4307–4319, http://dx.doi.org/10.1016/j.jeurceramsoc.2015.07.033.
[40] M. Vendrell-Saz, J. Molera, J. Roqué, J. Pérez-Arantegui, Islamic and Hispano-Moresque (múdejar) Lead Glazes in Spain: A Technical Approach, vol. 257, Geological Society, London, Special Publications, 2006, pp. 163–173, http://dx.doi.org/10.1144/GSL.SP.2006.257.01.13.
[41] S. Coentro, R.A.A. Trindade, J. Mirão, A. Candeias, L.C. Alves, R.M.C. Silva, V.S.F. Muralha, Hispano-Moresque ceramic tiles from the monastery of Santa Clara-a-Velha (Coimbra, Portugal), J. Archaeol. Sci. 41 (2014) 21–28, http://dx.doi.org/10.1016/j.jas.2013.07.031.
[42] A. Baricza, B. Bajnoczi, M. Szabo, M. Toth, Z. Bendo, C. Szabo, Deterioration of glazed architectural ceramics due to environmental factors: a comparative study of two buildings in Budapest, Earth Environ. Sci. 11 (2016) 449–462.
[43] E. Youssef, N. Mostafa, J.E. Khoury, T. Merhej, R. Lteif, Glaze surface defects causes and prevention controls, J. Ceram. Sci. Technol. (2022), http://dx.doi.org/10.4416/JCST2022-00003. Q5
[44] P. Colomban, B. Kırmızı, G. Simsek Franci, Cobalt and associated impurities in blue (and green) glass, glaze and enamel: relationships between raw materials, processing, composition, phases and international trade, Minerals 11 (2021) 633, http://dx.doi.org/10.3390/min11060633.
[45] J. Romero-Pastor, A. García-Porras, R. Van Grieken, S. Potgieter-Vermaak, J. Coll-Conesa, C. Cardell, New insights in technology characterization of medieval Valencia glazes: Medieval Valencia glazes, X-Ray Spectrom. 44 (2015) 426–435, http://dx.doi.org/10.1002/xrs.2613.
[46] Y. He, W. Li, Y. Zhai, L. Zhao, X. Lu, C. Xu, Research on the degradation mechanism of the lead-glazed cups from the 'Yangtze River estuary No. 2' shipwreck, Open Ceramics 14 (2023), http://dx.doi.org/10.1016/j.oceram.2023.100360, 100360.
[47] L. Maritan, C. Mazzoli, Phosphates in archaeological finds: implications for environmental conditions of burial, Archaeometry 46 (2004) 673–683, http://dx.doi.org/10.1111/j.1475-4754.2004.00182.x.
[48] L. Maritan, I. Angelini, G. Artioli, C. Mazzoli, M. Saracino, Secondary phosphates in the ceramic materials from Frattesina (Rovigo, North-Eastern Italy), J. Cult. Her. 10 (2009) 144–151, http://dx.doi.org/10.1016/j.culher.2008.01.008.
[49] P. Holakooei, A.H. Karimy, Colourants on the Persian architectural decorations from the 11th to the 15th century, Archaeometry 66 (2024) 600–617, http://dx.doi.org/10.1111/arcm.12951.
[50] L. Erkens, H. Hamers, R. Hermans, E. Claeys, M. Bijnens, Lead chromates: a review of the state of the art in 2000, Surf. Coat. Int. B Coat. Trans. 84 (2001) 169–176, http://dx.doi.org/10.1007/BF02700395.

Please cite this article in press as: C. Cardell, et al., Archaeometric analysis of Nasrid glazed architectural ceramics from the Alhambra and Generalife Monument, Granada (Spain), Bol. Soc. Esp. Cerám. Vidr. (2025), https://doi.org/10.1016/j.bsecv.2025.100477